ISSN 1070-3284, Russian Journal of Coordination Chemistry, 2022, Vol. 48, No. 5, pp. 301–310. © Pleiades Publishing, Ltd., 2022.
Russian Text © The Author(s), 2022, published in Koordinatsionnaya Khimiya, 2022, Vol. 48, No. 5, pp. 302–313.

Synthesis, Structure, and Photoluminescence of Zinc(II) and Silver(I) Complexes with 2-(3,5-Dimethyl-1*H*-pyrazol-1-yl)-4,6-Diphenylpyrimidine

K. A. Vinogradova[a], *, M. I. Rakhmanova[a], E. B. Nikolaenkova[b], V. P. Krivopalov[b], M. B. Bushuev[a], N. V. Pervukhina[a], D. Yu. Naumov[a], and S. A. Martynova[a]

[a] *Nikolaev Institute of Inorganic Chemistry, Siberian Branch, Russian Academy of Sciences, Novosibirsk, Russia*
[b] *Vorozhtsov Novosibirsk Institute of Organic Chemistry, Siberian Branch, Russian Academy of Sciences, Novosibirsk, Russia*
**e-mail: kiossarin@mail.ru*

Received November 3, 2021; revised November 26, 2021; accepted November 28, 2021

Abstract—The complexes $[AgL_2]PF_6$ (**I**) and $[ZnLCl_2]$ (**II**) (L = 2-(3,5-dimethyl-1*H*-pyrazol-1-yl)-4,6-diphenylpyrimidine) were prepared by the reaction of zinc(II) chloride or silver(I) hexafluorophosphate with L (M : L molar ratio of 1 : 1 or 1 : 2) in organic solvents. The structure of the complexes was determined by X-ray diffraction (CIF file CCDC no. 2118498). In both complexes, L is coordinated in the bidentate chelating manner; the coordination unit is a distorted tetrahedron. The coordination unit of **II** is formed by one coordinated molecule L and two chloride ions (ZnN_2Cl_2); in the case of silver(I), there are two molecules L (AgN_4). The photoluminescent properties of compounds **I** and **II** in the solid state were studied. The compound **II** shows fluorescence (1.3, 11 ns) in the blue spectral range (λ_{max} = 378 nm; quantum yield of 7.8%). The maximum at 530 nm in the photoluminescence spectrum of **I** is red-shifted by ~140–160 nm relative to the emission maxima of L and **II**. The complex **I** shows white light emission (1.6, 11 ns, quantum yield of 5.5%), which is due to intraligand transitions perturbed by the coordination of L to the silver atom. The photostability of **I** was studied at 300 and 80 K.

Keywords: white-light emitting luminophores, photostability, fluorescence, phosphorescence, coordination compounds

DOI: 10.1134/S1070328422050098

INTRODUCTION

Compounds emitting white light with chromaticity coordinates of approximately (0.33, 0.33) according to the International Commission on Illumination (CIE) are called white luminophores, and the devices based on them are called white-light emitting diodes (wLED). The devices emitting white light have important applications, for example, they are widely used in lighting fixtures. Therefore, the search and study of new compounds exhibiting efficient white photo- and electroluminescence is an important task.

There are two main approaches to obtaining white luminophores: the design of one-component (single emitting materials) and multicomponent emitters. One-component emitters include organic and coordination compounds that have a wide photoluminescence spectrum in the visible range, resulting in white emission [1, 2]. Multicomponent systems are fabricated using the following procedures: (1) doping of polymeric matrices with organic compounds that emit in red, green, and blue spectral ranges [2–5]; (2) deposition of organic layers emitting red, green, and blue light on one another [2]; (3) doping of organometallic coordination polymers with red, green, and blue fluorophores in a desired ratio [6–9]. A key problem of the use of multicomponent emitters in lighting devices is that various fluorophores often have different stabilities and, as a consequence, they can separately fail (burn down). This naturally disturbs the balance of components and generally deteriorates the white emission [10, 11]. In addition, their considerable drawback is that the emission color may depend on the voltage [11]. The systems that use one substance as a white light emitter are free from these drawbacks; therefore, they are promising for potential applications.

Currently, the following individual compounds able to emit white photoluminescence are known: zinc(II) and cadmium(II) complexes [12, 13], although they usually demonstrate blue emission [14–18], platinum complexes [19–22], rare examples of lanthanide complexes [23, 24], and some organic molecules [25–27]. Several recent publications describe the use of complexes of coinage metals such as copper(I) [28, 29], gold(I) [30], and silver(I) [31–33]. Some mechanisms of white luminescence were stud-

ied, for example, platinum(II) coordination compounds form exciplexes upon excitation; virtually simultaneous emission of the exciplex and the molecule gives rise to white luminescence [10, 22].

The ionic complex $[Ag(Dppb)_2]BF_4$ (Dppb = 1,2-bis(diphenylphosphino)benzene), which has a broad emission band with a maximum at 526 nm in the solid state was studied among other compounds in [32]. This complex was used as the only source of emission in a wLED device in the poly(vinylcarbazole) matrix. The fabricated device has a wider emission band than the initial complex: almost white luminescence (maximum brightness of 365 cd/m^2 at 20 V). It was shown [33] that white light emission can be obtained and wLED can be designed on the basis of silver(I) hybrid compound $[H_2DABCO][Ag_2X_4(DABCO)]$ (DABCO = 1,4-diazabicyclo[2.2.2]octane). Recently, we published a detailed study of two silver(I) nitrate complexes with 2-amino-4-phenyl-6-methylpyrimidine (Pym) [34]. At room temperature in the solid state, one of the described complexes ($[Ag_3(Pym)_2(H_2O)_{0.55}(NO_3)_3]$) showed white luminescence.

In this study, silver(I) complexes were also synthesized using a pyrimidine-based ligand, but with a pyrazole substituent present in position 2 of the pyrimidine ring, instead of the NH_2 group (Scheme 1). The resulting compound, 2-(3,5-dimethyl-1*H*-pyrazol-1-yl)-4,6-diphenylpyrimidine (L), mainly acts as a bidentate ligand, unlike the previously used Pym; this should promote the formation of mononuclear rather than polymeric compounds. It was also of interest to synthesize and study the photoluminescent (PL) properties of the zinc(II) complexes with the ligand L and to evaluate the applicability of this complex for obtaining white light emission.

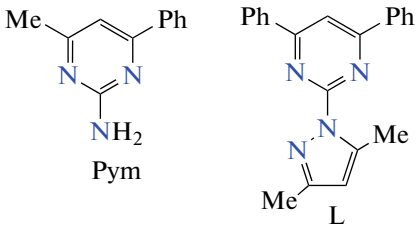

Scheme 1.

The purpose of this study is to synthesize silver(I) and zinc(II) complexes with L, determine the crystal structure of the complexes, and to study in detail their photoluminescent properties in the solid state.

EXPERIMENTAL

The complexes were synthesized using compound L (CAS 202192-87-8), silver(I) hexafluoroborate (CAS 26042-63-7), zinc(II) chloride (CAS 7646-85-7), dichloromethane, ethanol, and acetonitrile (all were reagent grade chemicals), which were commercially available and were used without additional purification. The absorption and PL spectra were recorded for solutions in dichloromethane (HPLC purity grade). Despite the fact that the compound L is commercially available, it can be synthesized by the reaction of 2-hydrazino-4,6-diphenylpyrimidine (CAS 76071-58-4) with acetylacetone (CAS 123-54-6) in an acidified ethanol solution by previously reported procedures [35, 36].

The elemental analysis (C, H, N) of complex **II** was carried out on a vario MICRO cube instrument using a standard procedure. The elemental analysis (C, H, N) of fluorine-containing complex **I** was carried out by a reported procedure [37].

For recording the diffuse reflectance spectra (DRS), samples of the complexes were mixed with barium sulfate in 1 : 100 ratio. The DRS were measured on a UV-3101 PC Shimadzu instrument. The spectra are presented as the Kubelka–Munk function, $F(R) = (1 - R)^2/2R$, where R is the diffuse reflectance coefficient of the sample in comparison with $BaSO_4$. The optical spectra for solutions were recorded on an SF-2000 spectrophotometer. Thermogravimetric analysis (TG) was carried out using a NETZSCH TG 209 F1 Iris Thermo Microbalance. X-ray powder diffraction (XRPD) study was perfomed on a Shimadzu XRD-7000 diffractometer (CuK_α radiation, Ni filter, Seller slits of 2.5°, and divergence slits of 0.5°) equipped with a DECTRIS MYTHEN2 R 1K detector.

The IR spectra of the complexes and the ligand were measured on a DIGILAB Scimitar FTS 2000 FTIR spectrometer in the 4000–400 cm^{-1} range and a Vertex 80 Bruker spectrometer in the 600–100 cm^{-1} range. The samples were ground in an agate mortar with dry KBr or polyethylene and pressed into pellets. The IR bands were assigned by comparison with published data [38, 39].

The stability of the silver(I) complex on exposure to light was studied using a laser diode emitting light at 405 nm (200 mV power). Samples of the complex were pressed in KBr pellets, the pellets were irradiated for a definite period of time, and then IR spectra were recorded in the 600–300 cm^{-1} range.

Synthesis of $[AgL_2]PF_6$ (I). A solution of $AgPF_6$ (23.2 mg, 0.0919 mmol) in acetonitrile (3.0 mL) was added to a solution of L (60.0 mg, 0.184 mmol) in dichloromethane (1.0 mL). A colorless transparent solution formed. When the solution volume decreased to ~2 mL, a white precipitate started to appear. The mixture was stirred for approximately 30 min at room temperature. The precipitate was filtered off on a glass porous filter, washed with acetonitrile, and dried in air. The yield was 57 mg (68%).

For $C_{42}H_{36}N_8F_6PAg$

Anal. calcd., %	C, 55.7	H, 4.0	N, 12.4
Found, %	C, 55.5	H, 3.8	N, 12.6

In a week, large, well-faceted colorless crystals appeared in the mother liquor. According to the single crystal X-ray diffraction data, the composition of the crystals was $[AgL_2]PF_6$.

Synthesis of a polycrystalline sample of $[ZnLCl_2]$ (II). A solution of $ZnCl_2$ (23.2 mg, 0.160 mmol) in ethanol (2 mL) was added to ligand L (40.2 mg, 0.123 mmol) in dichloromethane (2 mL). The resulting colorless transparent reaction mixture was stirred for 10 min at heating (T = 60°C); after that, a white polycrystalline product formed. The product was stirred with the mother liquor for 2 h with gentle heating (T = 35°C). The precipitate was filtered off, washed with dichloromethane (2 mL), and dried in air. The yield was 42 mg (74%).

For $C_{21}H_{18}N_4Cl_2Zn$			
Anal. calcd., %	C, 54.5	H, 3.9	N, 12.1
Found, %	C, 54.8	H, 3.8	N, 11.9

Synthesis of crystals of $[ZnLCl_2]$ (II). A solution of $ZnCl_2$ (7.0 mg, 0.051 mmol) in ethanol (2 mL) was added to a solution of ligand L (50.0 mg, 0.153 mmol) in ethanol (2 mL). The resulting colorless transparent reaction mixture was stirred for approximately 2 min at heating (T = 60°C), after that a white polycrystalline product is formed. The product was stirred with the mother liquor for 1 h. The precipitate was filtered off and washed with ethanol (1 mL). The yield was 23 mg (99%). Colorless transparent prismatic crystals appeared in the mother liquor 3 months later. According to the single crystal X-ray diffraction data, the composition of the crystals was $[ZnLCl_2]$.

For $C_{21}H_{18}N_4Cl_2Zn$			
Anal. calcd., %	C, 54.5	H, 3.9	N, 12.1
Found, %	C, 55.8	H, 4.3	N, 12.6

Single crystal X-ray diffraction study of compounds **I** and **II** was carried out at 150 K on a Bruker D8 Venture diffractometer equipped with a CMOS PHOTON III detector and an IμS 3.0 microfocus source (Montel focusing mirrors, MoK_α radiation). The reflection intensities were measured by φ and ω scanning of narrow (0.5°) frames. The data reduction was performed using the APEX3 program package [40]. The structures were solved by direct methods and refined by full-matrix least squares on F^2 in the anisotropic approximation for non-hydrogen atoms using the SHELXTL software package [41]. The hydrogen atoms of organic ligands were located from difference electron density maps and refined in the rigid body approximation. The crystal data and X-ray diffraction experiment details are summarized in Table 1.

Additional structural data for **I** and **II** are deposited with the Cambridge Crystallographic Data Centre (CCDC no. 2118498; deposit@ccdc.cam.ac.uk or http://www.ccdc.cam.ac.uk).

The photoluminescence and excitation spectra of the complexes in the solid state were recorded using a Horiba Fluorolog 3 spectrofluorimeter equipped with steady (450 W) and pulsed xenon lamps as light sources, a cooled detector, and double grating excitation and emission monochromators. The quantum yield was measured with a Fluorolog 3 spectrofluorimeter equipped with quantum sphere (Quanta-ϕ). The photoluminescence and excitation spectra were corrected for the source intensity (lamp and grating) and to the spectral response to emission (detector and grating) using standard correction curves. Temperature-dependent measurements were carried out using Optistat DN in the 77–300 K range.

The photoluminescence decay kinetics in the nanosecond time range was recorded by time-correlated single photon counting using a NanoLED pulsed light source and a NanoLED-C2 controller. Complex **I** was excited at 350 nm; and the emission was registrated at the 530 nm emission maximum; in the case of **II**, excitation was carried out at 300 nm and emission was registrated at 387 nm maximum (T = 300 K). The luminescence decay kinetics in the millisecond time range was measured using a pulsed xenon lamp (λ_{excit} = 320 nm, λ_{em} = 500 nm).

The photostability of $[AgL_2]PF_6$ was studied using two procedures.

Procedure 1. A fresh portion of the polycrystalline sample of complex **I** was placed between two quartz glasses, and its PL spectrum was recorded upon excitation at 360 nm. Next, the sample was irradiated successively with a set of wavelengths from 300 to 500 nm with a step of 10 nm (with this approach, the total irradiation time was ~10 min) and the emission spectrum was recorded once again at the initial parameters, and then two emission spectra, recorded before and after the irradiation, were compared.

Procedure 2. For an identical freshly prepared sample, 10 PL spectra were recorded in succession with excitation at 320 nm. In this case, the total irradiation time of the sample was 8 to 10 min depending on the range in which the emission spectra were recorded. The conclusion about the sample photostability was drawn from the change in the intensity of the PL spectrum both in the first and in the second procedures. Note that for substances that do not degrade under the action of electromagnetic radiation, the emission spectra do not change if they are recorded under the same conditions.

RESULTS AND DISCUSSION

The reaction between ligand L and silver(I) hexafluorophosphate in a CH_2Cl_2–MeCN (1 : 3) mixture results in the formation of a white polycrystalline precipitate (**I**, Scheme 2).

Table 1. Crystallographic data and structure refinement details for **I** and **II**

Parameter	Value	
	I	**II**
Molecular formula	$C_{42}H_{36}F_6N_8PAg$	$C_{21}H_{18}N_4Cl_2Zn$
M	905.63	462.66
System	Monoclinic	Monoclinic
Space group	$P2_1/c$	$C2/c$
a, Å	15.6308(3)	23.992(2)
b, Å	18.6760(4)	14.014(1)
c, Å	14.0639(2)	16.239(3)
β, deg	111.582(1)	131.286(2)
V, Å^3	3817.7(1)	4102.8(9)
Z	4	8
ρ(calcd.), g/cm^3	1.576	1.498
μ, mm^{-1}	0.643	1.472
F(000)	1840	1888
Crystal size, mm	0.12 × 0.08 × 0.08	0.15 × 0.10 × 0.04
Range of θ angles, deg	1.401–26.373	1.920–25.708
Number of measured reflections	50592	18927
Number of unique reflections	7812 (R_{int} = 0.0360)	3889 (R_{int} = 0.0611)
Completeness of data collection for θ = 25.00°, %	99.9	99.8
S-factor on F^2	1.048	1.068
R_1, wR_2 ($I > 2\sigma_I$)	0.0250, 0.0726	0.0546, 0.1414
R_1, wR_2 (all reflections)	0.0306, 0.0754	0.0729, 0.1526
Residual electron density, min/max, e/Å^3	0.323/–0.546	1.809/–0.630

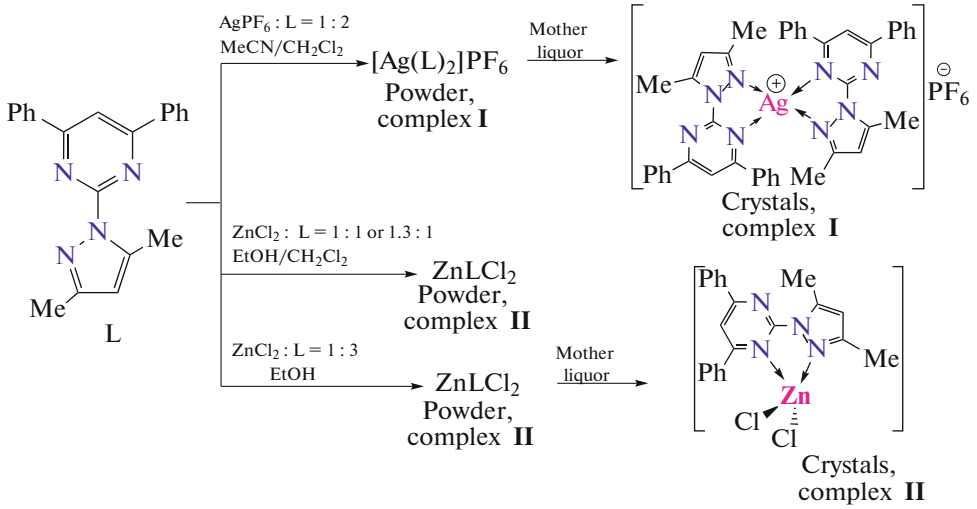

Scheme 2.

According to elemental analysis data, the obtained product had the composition AgL_2PF_6. In the mother liquor, large colorless transparent crystals suitable for the single crystal X-ray diffraction analysis appear within a week (Fig. S1). The calculated X-ray diffraction pattern derived from single crystal XRD data is in good agreement with experimental X-ray powder diffraction pattern of complex **I** (Fig. S2).

Complex **II** was obtained by the reaction of zinc(II) chloride with ligand L in ethanol (or in an EtOH–CH_2Cl_2 mixture) as a white powder, described as $ZnLCl_2$ according to elemental analysis data (see Scheme 2). This polycrystalline phase can also be obtained with other Zn : L molar ratios (1 : 1, 1.3 : 1, or 1 : 3), which was confirmed by XRPD (Fig. S3). The CHN analysis corresponding most closely to the theoretical one was obtained in the reaction with a minor excess of zinc(II) salt with respect to L (Zn : L = 1.3 : 1). This was due to the absence of L impurity in the sample of the complex. This sample was used subsequently for photophysical studies of complex **II**. The single crystals of **II** for X-ray diffraction were obtained from the mother liquor of the synthesis carried out at Zn : L ratio of 1 : 3. The calculated X-ray diffraction pattern derived from the single crystal XRD data coincides with the X-ray powder diffraction patterns for all isolated polycrystalline $ZnLCl_2$ samples (Fig. S3). This provided the conclusion that the same phase was formed in all cases.

The crystal structure of the complex **I** is formed by the $[AgL_2]^+$ and $[PF_6]^-$ ions. The structure of complex cation is shown in Fig. 1; the crystallographic data are summarized in Table 1. Two molecules L are coordinated to the silver atom in the bidentate chelating mode through the pyrazole N(2) atom and pyrimidine N(3) atom. The silver coordination polyhedron is a distorted tetrahedron. The bond lengths of **I** are summarized in Table 2. The pyrazole, pyrimidine, and phenyl rings are planar to within 0.01 Å. The planes of the pyrimidine rings are rotated relative to the pyrazole ring planes by 10.4° and 9.2°. The angles between the pyrimidine and phenyl ring planes are 21.4°, 37.1° and 26.9°, 34.8°, respectively. In the structure of **I**, intermolecular contacts are observed between the fluorine atoms of hexafluorophosphate anions and hydrogen atoms of the benzene rings of the $[AgL_2]^+$ complex cations; the F...H and F...C distances are approximately 2.3–2.5 Å and 3.1–3.3 Å, respectively.

The crystal structure of **II** is formed by the $ZnLCl_2$ molecules (Fig. 2, Table 1). The coordination mode of L is the same as in complex **I**. Zinc coordinates one molecule L; the zinc coordination polyhedron is completed by chlorine atoms to a distorted tetrahedron. The coordination of ligand L results in formation of a nearly planar ZnN_3C five-membered chelate ring, with the Zn(1) atom deviating from the mean chelate plane by –0.0092 Å. The bond lengths for **II** are given in Table 2. The pyrazole, pyrimidine, and phenyl rings are planar to within 0.01 Å. The angles between the pyrimidine and phenyl ring planes are 7.6° and 46.5°; the plane of the pyrimidine ring is rotated relative to the pyrazole ring plane by 4.1°. In the structure of **II**, intermolecular contacts are observed between the chlorine atoms and the hydrogen atoms of the pyrazole and phenyl rings of neighboring molecules; the Cl...H distances are approximately 2.7–2.8 Å, and the Cl...C distances are 3.4–3.6 Å. Worthy of note is the π-stacking interaction between the centers of the pyrazole and phenyl rings of neighboring molecules, arranged parallel to each other in the crystal structure, with the distance between the planes being approximately 3.490 Å. The distance between the centroids of these rings is 3.682 Å. (Fig. S4). The bond lengths and angles in the complexes are in good agreement with reported data [42].

The IR spectra of **I** and **II** are measured and analyzed in the range from 4000 to 100 cm^{-1} (Figs. S5 and S6). The basic vibrations of the complexes and the ligand L are presented in Table 3. The vibrations of CH and CH_3 groups and the stretching-bending vibrations of the rings in the IR spectra of the complexes **I** and **II** are slightly shifted relative to the corresponding vibrations in the spectrum of L. The vibration mode at 840 cm^{-1} found in the spectrum of **I** corresponds to the uncoordinated PF_6^- ion. In the low-frequency region, new bands appear in the spectra of the complexes compared with the spectrum of L, while some bands disappear. In the IR spectrum of the complex **II**, the Zn–N and Zn–Cl bands are located in the same range (345–310 cm^{-1}), which complicates their assignment. Presumably, the bands at 343, 336, and 315 cm^{-1}, which are absent in the spectra of L, correspond to stretching modes in the ZnN_2Cl_2 coordination unit. The Ag–N mode is weaker in the IR spectrum of **I** than in the IR spectrum of **II** and is located at 336 cm^{-1}.

The photoluminescent properties of complexes **I** and **II** were studied in the solid state at room temperature; for complex **I**, studies were also carried out at temperatures between 77 and 300 K. Note that for ligand L and the complexes, absorption spectra in dichloromethane were recorded (Fig. S7). An absorption spectra of the complexes are almost identical to the spectrum of L; no metal–ligand charge transfer bands were found above 350 nm, indicating that the complexes dissociate almost completely in solution. For the ligand L, photophysical characteristics in solutions were obtained. The ligand L shows one emission band at 380 nm with an excited state lifetime of 6.8 ns (Fig. S8) and a quantum yield of 0.4% (λ_{excit} = 320 nm).

Compound **II** has a blue emission which is typical for zinc(II) complexes [14–18]; the PL band in the spectrum of **II** (λ_{em} = 387 nm) is red-shifted with respect to the PL band of L (λ_{em} = 368 nm) by 19 nm (Fig. 3). Generally, the PL spectrum of **II** resembles the PL spectrum of L (λ_{em} = 368 nm). The emission band at 387 nm has two excited state lifetimes (t_1 = 1.6 ns, t_2 = 11 ns, Table 4, Fig. S9); the contribution of the first time is less than 0.01%, which can be caused by the relaxation of excited surface molecules. Similar positions of the maxima in the PL spectra of **II** and L (387 and 368 nm) and similar nanosecond lifetimes

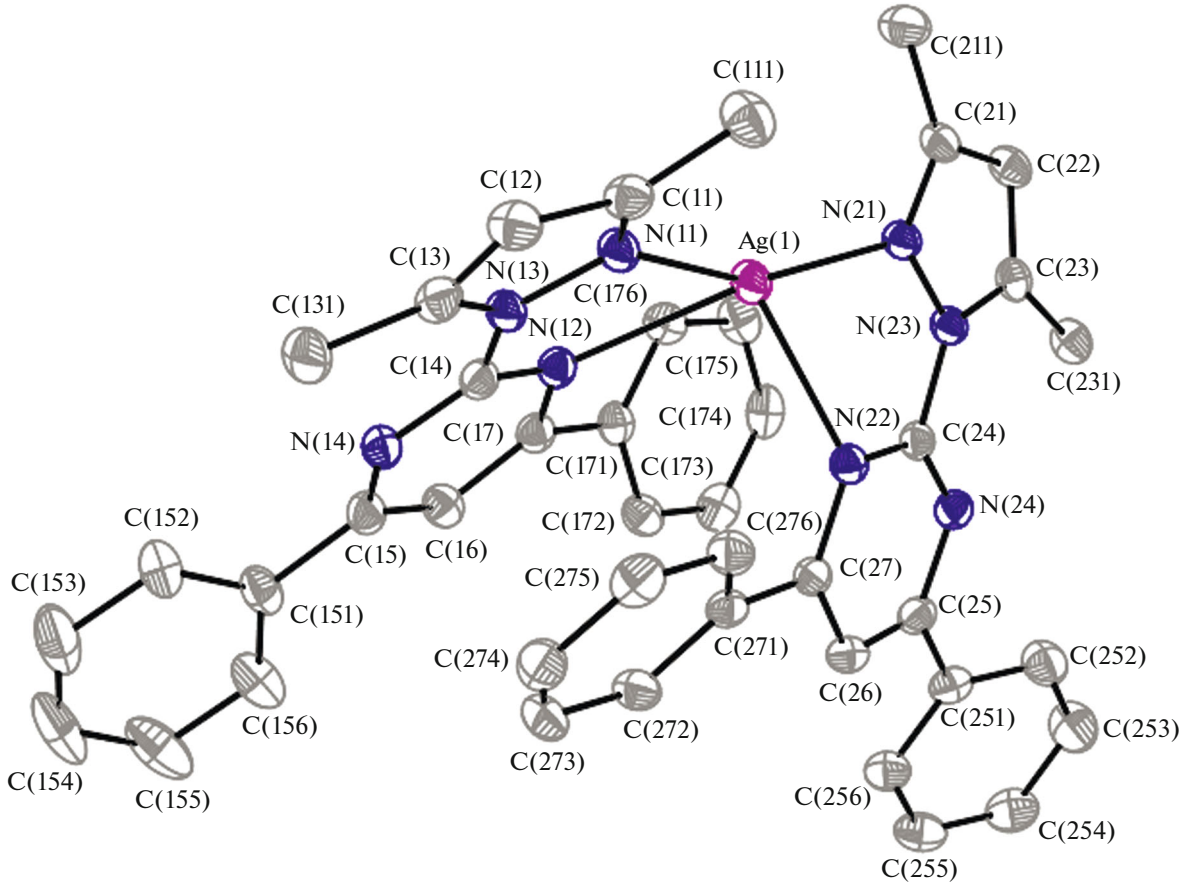

Fig. 1. Structure of the $[AgL_2]^+$ complex cation.

(11 and 9.1 ns) apparently indicate that the nature of emission of **II** is related to intraligand transitions of the coordinated molecule L. The quantum yield of PL of **II** is higher by an order of magnitude (Table 4), which is due to the formation of more rigid and planar $[ZnLCl_2]$ molecule.

Complex **I** exhibits almost white luminescence upon photoexcitation at various wavelengths (λ_{excit} = 320, 340, 360, 390 nm) (Fig. 4, Fig. S10, Table S1). For example, after excitation at 390 nm, the chromaticity of the emitted light corresponds to the 0.30; 0.37 point in the CIE coordinates. The PL spectrum of complex **I** shows one broad band with a maximum at 500–540 nm with a vibrational structure; the excitation spectrum also shows a vibrational structure. The emission band of **I** has two nanosecond lifetimes (Table 4, Fig. S11), which are close to the lifetimes of **II** and L. Apparently, the emission of **II** is due to intraligand transitions strongly perturbed by the coordinated silver atom.

It is known that silver(I) compounds can be unstable on exposure to light; therefore, one of the goals of the study was to assess the stability of the obtained complex **I** under the action of electromagnetic radiation with different energies. The photostability of **I** was studied at 300 and 77 K under irradiation at different wavelengths (Figs. S12–S16). At room temperature, the complex decomposes rather rapidly under the action of light (Figs. S12, S13). After 10 min, the intensity of the main PL band decreases by approximately 15% (Fig. S12), but with gradual decrease in the PL intensity, the shape of the emission line is retained (Fig. S13). After 2 h of irradiation, the PL spectrum virtually disappears (Fig. S14). The destruction of the complex may be associated with the destruction of the coordination bond and reduction of Ag^+ to Ag^0. Therefore, it can be concluded than irradiation induces more intense destruction of the luminescent silver(I) complex (φ = 5.5%) compared to the less luminescent ligand L (φ = 0.5%); this decreases the intensity of the PL band in the spectrum. We attempted to observe this process by IR spectroscopy. The photostability of complex **I** was studied in the range of 600–300 cm^{-1}, since the greatest number of differences between the spectrum of **I** and the spectrum of L is concentrated in this range (Fig. S6). A KBr pellet of **I** was irradiated with a laser at λ = 405 nm for various periods of time, and then the IR spectrum was recorded. This was not accompanied by any changes in the IR spectrum of **I** (Fig. S17), which indi-

Table 2. Selected interatomic distances (Å) in structures **I** and **II**

Bond *d*, Å		Bond *d*, Å	
I		**II**	
Coordination unit			
Ag(1)–N(11)	2.180(1)	Zn(1)–N(1)	2.038(4)
Ag(1)–N(21)	2.181(1)	Zn(1)–N(3)	2.113(3)
Ag(1)–N(12)	2.478(1)	Zn(1)–Cl(1)	2.217(1)
Ag(1)–N(22)	2.477(1)	Zn(1)–Cl(2)	2.204(1)
Pyrazole rings			
N–N	1.373(2), 1.378(2)	N–N	1.379(4)
N–C	1.323(2)–1.380(2)	N–C	1.330(5), 1.374(5)
C–C	1.363(2)–1.409(2)	C–C	1.364(6), 1.403(6)
$C–C_{Me}$	1.487(2)–1.492(2)	$C–C_{Me}$	1.483(6), 1.485(6)
Pyrimidine ring			
N–C	1.318(2)–1.350(2)	N–C	1.315(5)–1.366(5)
C–C	1.386(2)–1.391(2)	C–C	1.381(6), 1.387(6)
$C–C_{Ph}$	1.478(2)–1.484(2)	$C–C_{Ph}$	1.478(5), 1.466(5)
Phenyl rings			
1.374(3)–1.401(2)		1.368(7)–1.416(6) Å	
Intermolecular contacts			
F(5)...H(172)' 2.518	F(5)...C(172)' 3.301	Cl(1)...H(56)' 2.804	Cl(1)...C(56)' 3.485
F(5)...H(256)' 2.427	F(5)...C(256)' 3.256	Cl(1)...H(2)' 2.773	Cl(1)...C(2)' 3.565
F(1)...H(272)' 2.368	F(1)...C(272)' 3.165	Cl(2)...H(73)' 2.872	Cl(2)...C(73)' 3.606

Table 3. Main vibrational frequencies in the IR spectra of the ligand L and the complexes **I** and **II**

Compound	ν(CH), cm^{-1}	ν(CH_3), cm^{-1}	$(\nu + \delta)_{rings}$	ν(P–F)	ν(M–N)	ν(M–Cl)
L	3080 3045	2981, 2924	1604, 1592, 1578, 1570, 1531, 1499			
I	3142 3110 3096 3060	2971, 2922	1602, 1594, 1577, 1567, 1527, 1498	840	336	
II	3146 3117 3090 3063	2986, 2926, 2849	1602, 1594, 1577, 1570, 1531, 1523		343, 336, 315 (mixed with Zn–Cl)	343, 336, 315 (mixed with Zn–N)

cates that the changes of molecules of **I** involve only the surface of the sample. Note that both complexes are thermally stable up to 300°C (Figs. S18 and S19).

At 77 K, the complex **I** is photostable. Figure S15 shows the curves for luminescence intensity versus time (λ_{em} = 540 nm) upon excitation at 360 nm; it can be seen that the intensity remains invariable. Figure S16 presents a comparison of the spectra before and after irradiation. For the complex **I**, the PL and excitation spectra were recorded and the lifetimes were measured at various temperatures (Fig. 5 and Fig. S20). As the temperature is lowered, a new line with its own vibrational structure appears in the PL spectrum. The lifetimes, which increase by six orders of magnitude (0.16 ms, 4.8 ms, Table 4), indicate the appearance of a new emission mechanism associated with the

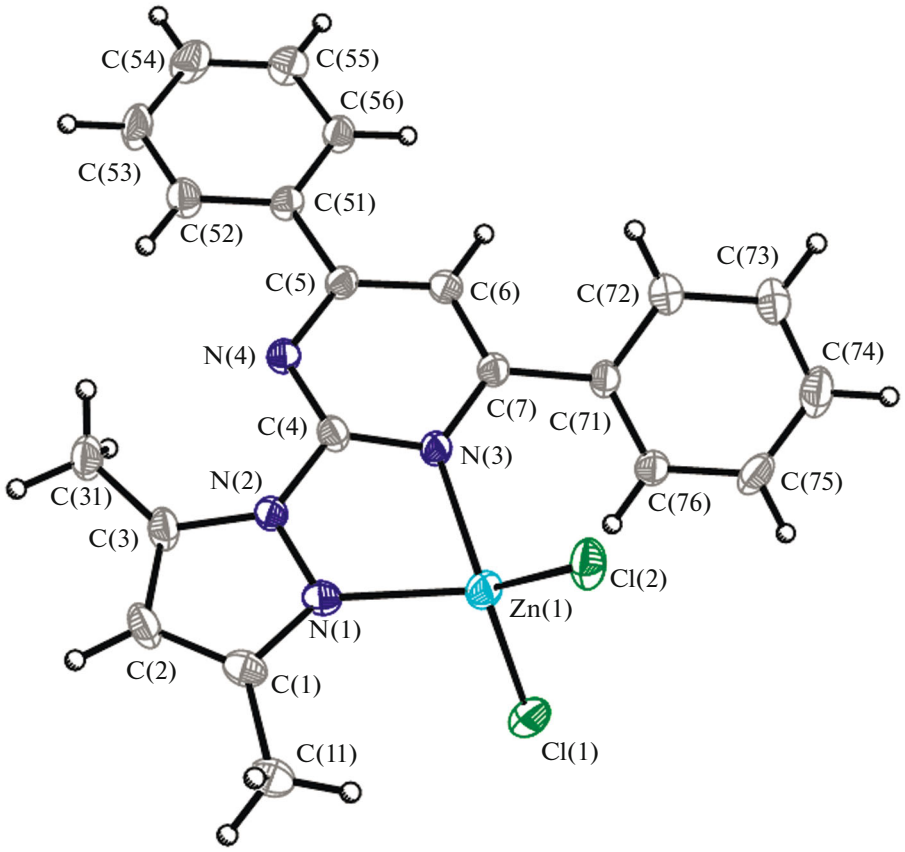

Fig. 2. Structure of the $[ZnLCl_2]$ complex.

relaxation of triplet states. This mechanism can be related to charge transfer excited states (MLCT).

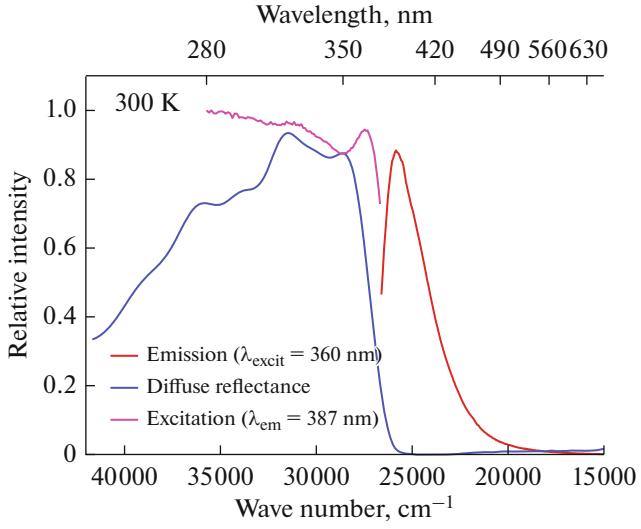

Fig. 3. Photoluminescence, excitation, and diffuse reflectance spectra of the complex **II** at 300 K.

Silver(I) and zinc(II) chelate complexes with 2-(1*H*-pyrazol-1-yl)pyrimidine derivative were synthesized and structurally characterized. In both complexes, the 2-(1*H*-pyrazol-1-yl)pyrimidine core is coordinated bidentately, giving rise to mononuclear $[AgL_2]PF_6$ and $[ZnLCl_2]$ complexes.

As a rule, organic molecules containing aromatic carbocyclic and heterocyclic moieties luminesce due to n–π* and π–π* transitions, which naturally lead to blue luminescence. It is quite expectable that the used ligand L shows blue emission. While considering the formation of zinc(II) and silver(I) complexes with L, we compared the influence of metal coordination on the PL behavior of molecule L. At room temperature, both complexes possess fluorescence, the coordination of zinc(II) ion does not strongly perturb the levels of the ligand, and the $[ZnLCl_2]$ complex shows blue emission, similar to that of the ligand L, but with a higher quantum yield. Meanwhile, the coordination of silver(I) ion, presumably, introduces a much greater perturbation to the orbitals of the coordinated ligand, which induces a pronounced shift and broadening of the PL band. The resulting broad band covers the whole visible range, which generates white luminescence.

Table 4. Photophysical data for ligand L and complexes **I** and **II** in the solid state

Compound	Maximum in the PL spectrum	Quantum yield	Excited state lifetime
L	368 nm (λ_{excit} = 340 nm, 300 K)	0.5% (λ_{excit} = 340 nm, 300 K)	t = 9.1 ns (λ_{excit} = 300 nm, λ_{em} = 380 nm, 300 K)
I	408, 435, 530 nm (λ_{excit} = 360 nm, 300 K)	Not less than 5.5% (λ_{excit} = 360 nm, 300 K)	t_1 = 2.8 ns, t_2 = 12 ns (λ_{excit} = 350 nm, λ_{em} = 530 nm, 300 K)
	455, 485, 520 nm (λ_{excit} = 360 nm, 77 K)		t_1 = 0.16 ms, t_2 = 4.8 ms (λ_{excit} = 320 nm, λ_{em} = 500 nm, 77 K)
II	387 nm (λ_{excit} = 340 nm, 300 K)	7.8% (λ_{excit} = 320 nm, 300 K)	t_1 = 1.3 ns, t_2 = 11 ns (λ_{excit} = 300 nm, λ_{em} = 387 nm, 300 K)

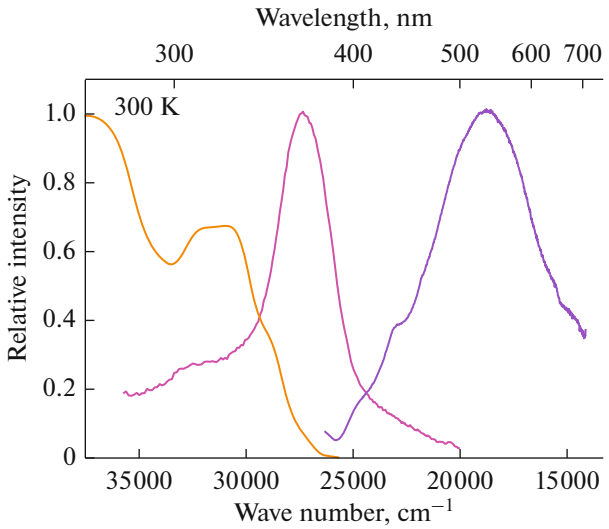

Fig. 4. Photolumiunescence (λ_{excit} = 360 nm purple line), excitation (λ_{em} = 530 nm pink line), and diffuse reflectance spectra (orange line) of the complex **I** at 300 K.

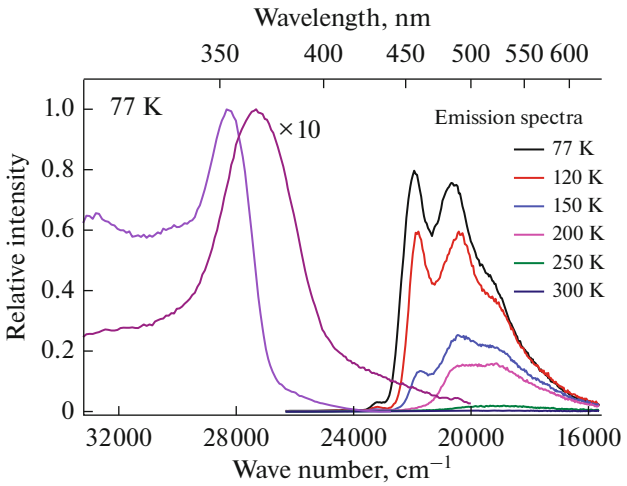

Fig. 5. Photolumiunescence spectra at various temperatures (λ_{excit} = 360 nm) and excitation spectra at 77 (λ_{em} = 455 and 530 nm) for the complex **I**.

ACKNOWLEDGMENTS

The authors are grateful to T.S. Sukhikh for providing the data measured at the X-ray diffraction Center for Collective Use of the Institute of Inorganic Chemistry, Siberian Branch, Russian Academy of Sciences, to I.V. Yushina for recording the diffuse reflectance spectra, to A.A. Shapovalova for measuring the IR spectra, to A.P. Zubareva for CHN analysis, to P.E. Plyusnin for thermogravimetric analysis, and to A.O. Matveeva for measuring the X-ray diffraction patterns.

FUNDING

This study was supported by a grant of President of the Russian Federation for young scientists (project no. MK-1219.2020.3) and by the Ministry of Science and Higher Education of the Russian Federation (project nos. 121031700315-2, 121031700321-3, 121031700314-5, and 121031700313-8).

CONFLICT OF INTEREST

The authors declare that they have no conflicts of interest.

SUPPLEMENTARY INFORMATION

The online version contains supplementary material available at https://doi.org/10.1134/S1070328422050098.

REFERENCES

1. Gaffuri, P., Stolyarova, E., Llerena, D., et al., *Renewable and Sustainable Energy Rev.*, 2021, vol. 143, p. 110869. https://doi.org/10.1016/j.rser.2021.110869
2. Chen, S.-A. and Chang, E.-C., in *Semiconducting Polymers*, Hsieh, B.R. and Wei, Y, Eds., Washington: American Chemical Society, 1999, Ch. 11, p. 163. https://doi.org/10.1021/bk-1999-0735.ch011
3. Kim, H.U., Jang, J.-H., Park, H.J., et al., *J. Nanosci. Nanotechnol.*, 2017, vol. 17, p. 5587. https://doi.org/10.1166/jnn.2017.14155

4. Hao, Z., Jiang, H., Liu, Y., et al., *Tetrahedron*, 2016, vol. 72, p. 8542. https://doi.org/10.1016/j.tet.2016.11.008
5. Zeng, Q., Li, F., Chen, Z., et al., *ACS Appl. Mater. Interfaces*, 2020, vol. 12, p. 4649. https://doi.org/10.1021/acsami.9b18162
6. Su, H.-C., Chen, Y.-R., and Wong, K.-T., *Adv. Funct. Mater.*, 2020, vol. 30, p. 1906898. https://doi.org/10.1002/adfm.201906898
7. Tang, Y., Wu, H., and Cao, W., *Adv. Opt. Mater.*, 2020, p. 2001817. https://doi.org/10.1002/adom.202001817
8. Zhang, N., Guan, Q.-L., Liu, C.-H., et al., *Appl. Organomet. Chem.*, 2020, p. e5506. https://doi.org/10.1002/aoc.5506
9. Seetha Lekshmi, S., Ramya, A.R., Reddy, M.L.P., and Varughese, S., *J. Photochem. Photobiol.*, 2017, vol. 33, p. 109.
10. Fleetham, T. and Li, J., *J. Photon. Energy*, 2014, vol. 4, pp. 040991-1. https://doi.org/10.1117/1.JPE.4.040991
11. Chen, Z., Ho, C.-L., Wang, L., and Wong, W.-Y., *Adv. Mater.*, 2020, vol. 32, p. 1903269. https://doi.org/10.1002/adma.201903269
12. Kim, D.-E., Shin, H.-K., Kim, N.-K., et al., *J. Nanosci. Nanotechnol.*, 2014, vol. 14, p. 1019. https://doi.org/10.1166/jnn.2014.9140
13. Hao, Y., Meng, W., Xu, H., et al., *Org. Electronics*, 2011, vol. 12, p. 136. https://doi.org/10.1016/j.orgel.2010.10.019
14. Wang, S., *Coord. Chem. Rev.*, 2001, vol. 215, p. 79. https://doi.org/10.1016/S0010-8545(00)00403-3
15. Erxleben, A., *Coord. Chem. Rev.*, 2003, vol. 246, p. 203. https://doi.org/10.1016/S0010-8545(03)00117-6
16. Zheng, S.-L. and Chen, X.-M., *Aust. J. Chem.*, 2004, vol. 57, p. 703. https://doi.org/10.1071/CH04008
17. Yu, C., Wang, X., Wu, T., et al., *Dalton Trans.*, 2020, vol. 49, p. 12082. https://doi.org/10.1039/D0DT02033H
18. Miao, J., Nie, Y., Li, Y., et al., *J. Mater. Chem.*, 2019, vol. 7, p. 13454. https://doi.org/10.1039/C9TC04033A
19. Zhu, L., Xie, W., Qian, C., et al., *Adv. Opt. Mater.*, 2020, vol. 8, p. 2000406. https://doi.org/10.1002/adom.202000406
20. Jaime, S., Arnal, L., Sicilia, V., and Fuertes, S., *Organometallics*, 2020, vol. 39, p. 3695. https://doi.org/10.1021/acs.organomet.0c00510
21. Sukhikh, T.S., Khisamov, R.M., Bashirov, D.A., et al., *Cryst. Growth Des.*, 2020, vol. 20, p. 5796. https://doi.org/10.1021/acs.cgd.0c00406
22. Wu, J., Ameri, L., Cao, L., and Li, J., *Appl. Phys. Lett.*, 2021, vol. 118, p. 073301. https://doi.org/10.1063/5.0043955
23. Boddula, R., Tagare, J., Singh, K., and Vaidyanathan, S., *Mater. Chem. Front.*, 2021, vol. 5, p. 159. https://doi.org/10.1039/D1QM00083G
24. Ilmi, R., Khan, M.S., Sun, W., et al., *J. Mater. Chem.*, 2019, vol. 7, p. 13966. https://doi.org/10.1039/C9TC04653D
25. Ma, X., Jia, L., Yang, B., et al., *J. Mater. Chem.*, 2021, vol. 9, p. 727. https://doi.org/10.1039/D0TC04234J
26. Liu, X., Wang, Y.-F., Li, M., et al., *Org. Electron.*, 2021, vol. 88, p. 106017. https://doi.org/10.1016/j.orgel.2020.106017
27. Khammultri, P., Kitisriworaphan, W., Chasing, P., et al., *Polym. Chem.*, 2021, vol. 12, p. 1030. https://doi.org/10.1039/D0PY01541E
28. Lian, L., Zhang, P., Liang, G., et al., *ACS Appl. Mater. Interfaces*, 2021, vol. 13, p. 22749. https://doi.org/10.1021/acsami.1c03881
29. Wu, T.-C., Zhao, F.-Z., Hu, Q.-L., et al., *Appl. Organomet. Chem.*, 2020, vol. 34, p. e5691. https://doi.org/10.1002/aoc.5691
30. Wang, X.-Y., Hu, Y.-X., Yang, X.-F., et al., *Org. Lett.*, 2019, vol. 21, p. 9945. https://doi.org/10.1021/acs.orglett.9b03875
31. Xue, Z.-Z., Meng, X.-D., Li, X.-Y., et al., *Inorg. Chem.*, 2021, vol. 60, p. 4375. https://doi.org/10.1021/acs.inorgchem.1c00280
32. Kaeser, A., Moudam, O., Accorsi, G., et al., *Eur. J. Inorg. Chem.*, 2014, vol. 2014, p. 1345. https://doi.org/10.1002/ejic.201301349
33. Sun, C., Guo, Y.-H., Yuan, Y., et al., *Inorg. Chem.*, 2020, vol. 59, p. 4311. https://doi.org/10.1021/acs.inorgchem.9b03139
34. Shekhovtsov, N.A., Vinogradova, K.A., Berezin, A.S., et al., *Inorg. Chem. Front.*, 2020, vol. 7, p. 2212. https://doi.org/10.1039/D0QI00254B
35. Bushuev, M.B., Krivopalov, V.P., Semikolenova, N.V., et al., *Russ. J. Coord. Chem.*, 2006, vol. 32, p. 199. https://doi.org/10.1134/s1070328406030067
36. Sedova, V.F., Shkurko, O.P., Nekhoroshev, S.A., et al., *Heterocycl. Comp.*, 2003, vol. 34. https://doi.org/10.1002/CHIN.200304150
37. Fadeeva, V.P., Tikhova, V.D., Nikulicheva, O.N., et al., *J. Analyt. Chem.*, 2008, vol. 63, p. 1197. https://doi.org/10.1134/S1061934808110142
38. Nakamoto, K., *Infrared and Raman Spectra Of Inorganic and Coordination Compounds, Applications in Coordination, Organometallic, and Bioinorganic Chemistry*, New Jersey: Wiley, 2014, p. 408.
39. Vinogradova, K.A., Plyusnin, V.F., Kupryakov, A.S., et al., *Dalton Trans.*, 2014, vol. 43, p. 2953. https://doi.org/10.1039/C3DT53040J
40. *Bruker Apex3 Software Suite. Apex3, SADABS-2016/2 and SAINT. Version 2019.1-0*, Madison: Bruker AXS Inc., 2017.
41. Sheldrick, G.M., *Acta Crystallogr., Sect. C: Struct. Chem.*, 2015, vol. 71, p. 3. https://doi.org/10.1107/S2053273314026370
42. Allen, F.H., Kennard, O., and Watson, D.G., *J. Chem. Soc., Perkin Trans.*, 1987, no. 12, p. S1. https://doi.org/10.1039/p298700000s1

Translated by Z. Svitanko